

Fixed-Gain AF Relaying for RF-THz Wireless System over α - κ - μ Shadowed and α - μ Channels

Pranay Bhardwaj, *Graduate Student Member, IEEE* and S. M. Zafaruddin, *Senior Member, IEEE*

Abstract—Recent research investigates the decode-and-forward (DF) relaying for mixed radio frequency (RF) and terahertz (THz) wireless links with zero-boresight pointing errors. In this letter, we analyze the performance of a fixed-gain amplify-and-forward (AF) relaying for the RF-THz link to interface the access network on the RF technology with wireless THz transmissions. We develop probability density function (PDF) and cumulative distribution function (CDF) of the end-to-end SNR for the relay-assisted system in terms of bivariate Fox's H function considering α - μ fading for the THz system with non-zero boresight pointing errors and α - κ - μ shadowed (α -KMS) fading model for the RF link. Using the derived PDF and CDF, we present exact analytical expressions of the outage probability, average bit-error-rate (BER), and ergodic capacity of the considered system. We also analyze the outage probability and average BER asymptotically for a better insight into the system behavior at high SNR. We use simulations to compare the performance of the AF relaying having a semi-blind gain factor with the recently proposed DF relaying for THz-RF transmissions.

Index Terms—Amplify-and-forward, bit-error-rate, DF, ergodic capacity, performance analysis, pointing errors, terahertz.

I. INTRODUCTION

Terahertz (THz) communication is an emerging technology for backhaul/fronthaul applications for next-generation wireless networks [1], [2]. The THz link is less susceptible to the signal interference and can provide enormous unlicensed bandwidth to support high capacity links for broadband access in small cells and cell-free networks. However, the THz signal transmissions behave differently from the conventional radio frequency (RF) since the THz link is subjected to random pointing errors caused by the misalignment between transmitter and receiver antenna beams and incurs hardware impairments at higher frequencies in addition to the signal fading and path loss [3]. At the physical layer, an integration of line-of-sight THz transmissions for fronthauling and radio frequency (RF) connectivity for the end-users can be a viable system configuration for 6G wireless networks, especially in difficult terrains.

Cooperative relaying is an efficient technique to increase the data rate and extend the coverage range of wireless transmissions. The use of relaying at THz frequencies has recently been studied [4]–[12]. The authors in [6] presented the outage probability of a dual-hop THz-THz link using the decode-and-forward (DF) relaying protocol. Recently, the authors in [8], [9] considered the DF relaying protocol to facilitate data transmissions between the THz-RF mixed link. They have developed outage probability, average bit-error-rate (BER), and ergodic capacity performance for THz-RF transmissions by deriving probability density function (PDF)

and cumulative distribution function (CDF) of the THz link in terms of incomplete Gamma function over α - μ fading with zero-boresight pointing errors. It is a well-known fact that the fixed-gain amplify-and-forward (AF) relaying possesses desirable characteristics of lower computational complexity and does not require continuous monitoring of the channel state information (CSI) for decoding at the relay [13]. There is limited research on AF relaying for THz systems. The authors in [10] considered an AF relay for nano-scale THz transmissions without considering the effect of short-term fading. Considering Rayleigh fading, [11] studied an AF-assisted cooperative In-Vivo nano communication at THz frequencies. The authors in [14] analyzed the THz-THz dual-hop system with fixed-gain relaying considering zero-boresight pointing errors. It should be mentioned that the AF relaying has been extensively studied for various wireless technologies such as RF-RF [13], [15], RF-free space optics (FSO) [16], [17], RF-power line communications (PLC) [18], mmWave-FSO [19], [20], PLC-visible light communications (VLC) [21], and RF-underwater wireless communications (UWOC) [22].

In this letter, we analyze the performance of a mixed RF-THz wireless system assisted by a fixed-gain AF relaying by considering non-zero boresight pointing errors with α - μ fading for the THz and generalized α - κ - μ shadowed (α -KMS) fading [23] for the RF link. To the best of the authors' knowledge, generalized pointing errors has not yet been considered for the THz link and the use of α -KMS has not been studied for the dual-hop relaying for mixed systems. It should be mentioned that a recent measurement campaign validates α - μ distribution for the short-term fading at 152 GHz for a link length within 50 m [24]. We list the major contributions of the paper as follows:

- We provide statistical results on the signal-to-noise ratio (SNR) by deriving PDF and CDF of the THz link under the joint effect of deterministic path-loss, α - μ short-term fading, and generalized pointing errors model. The derived PDF and CDF are also valid for real-valued α and μ parameters and are represented in terms of Meijer's G function for an elegant performance analysis with the zero-boresight model as a special case.
- Using the derived PDF and CDF of the THz link, we derive novel density and distribution functions of the end-to-end SNR for the RF-THz mixed link integrated with a fixed-gain AF relay.
- We develop exact analytical expressions of outage probability, average BER, and ergodic capacity of the relay-assisted system in terms of bivariate Fox's function. By computing residues of Fox's H function at each pole, we also provide asymptotic expressions for the outage probability and the average BER at high SNR in terms of simpler Gamma functions, and derive the diversity order of the system.

II. SYSTEM MODEL

We consider a mixed fronthaul/radio access system for uplink data transmissions where a fixed-gain AF relay facili-

This work was supported in part by the Science and Engineering Research Board (SERB), Department of Science and Technology (DST), Government of India, under Start-up Research Grant SRG/2019/002345.

Pranay Bhardwaj (p20200026@pilani.bits-pilani.ac.in) and S. M. Zafaruddin (syed.zafaruddin@pilani.bits-pilani.ac.in) are with the Department of Electrical and Electronics Engineering, Birla Institute of Technology and Science, Pilani, Pilani-333031, Rajasthan, India.

tates communication between the source and destination. We establish broadband radio access from the source to the relay over RF and fronthaul link from the relay to the destination over THz. The relay includes a frequency up-converter to generate THz signals from a low-frequency RF. There is no direct link between the source and destination since both THz and RF operate on different carrier frequencies. The THz link is subjected to pointing errors in addition to the path gain, short-term fading, and hardware impairments of the transmitter and receiver.

In the first hop, the received signal y_R^1 at the relay is expressed as $y_R = H_r h_{fr} S + w_r$, where S is the transmitted signal from the source, w_r is the additive white Gaussian noise (AWGN) signal with variance $\sigma_{w_r}^2$, H_r is the RF channel path-gain, and h_{fr} is the fading coefficient. We use the generalized α - κ - μ shadowed (a.k.a α -KMS) distribution to model the short term fading $|h_{fr}|$ for the RF link with PDF [23]:

$$f_{|h_{fr}|}(x) = \frac{m_r^{m_r} \alpha_r}{2c_r^{\mu_r} \Gamma(\mu_r)(\mu_r \kappa_r + m_r)_r m_r \bar{\gamma}_r} \left(\frac{x}{\bar{\gamma}_r}\right)^{\frac{\alpha_r \mu_r}{2} - 1} \exp\left(-\frac{1}{c} \left(\frac{x}{\bar{\gamma}_r}\right)^{\frac{\alpha_r}{2}}\right) {}_1F_1\left(m_r, \mu_r; \frac{\mu_r \kappa_r}{c(\mu_r \kappa_r + m_r)} \left(\frac{x}{\bar{\gamma}_r}\right)^{\frac{\alpha_r}{2}}\right) \quad (1)$$

where $\{\alpha_r, \kappa_r, \mu_r, m_r\}$ are the fading parameters, ${}_1F_1$ is the confluent Hypergeometric function and the parameter c is defined in [23]. In the second hop, the relay amplifies the incoming signal y_R with a gain \mathcal{G} to get the received signal at the destination (assuming negligible hardware distortions [8], [9]) $y_D = H_t h_p h_{ft} \mathcal{G} y_R + w_t$, where H_t is the path gain of THz link, w_t is the AWGN with variance $\sigma_{w_t}^2$, h_p models pointing errors, and $|h_{ft}|$ is the short-term fading of the THz link with PDF:

$$f_{|h_{ft}|}(x) = \frac{\alpha_t \mu_t}{\Omega^{\alpha_t \mu_t} \Gamma(\mu_t)} x^{\alpha_t \mu_t - 1} \exp\left(-\frac{\mu_t}{\Omega} x^{\alpha_t}\right) \quad (2)$$

where $\{\alpha_t, \mu_t, \Omega\}$ are the fading parameters for the THz link, and $\Gamma(\cdot)$ denotes the Gamma function. We use the generalized non-zero boresight statistical model for h_p [25]:

$$f_{h_p}(h_p) = \frac{\phi \exp\left(\frac{-s^2}{2\sigma^2}\right) h_p^{\phi-1} I_0\left(\frac{s}{\sigma^2} \sqrt{\frac{w_{zeq}^2 \ln \frac{S_0}{h_p}}{2}}\right)}{A_0^\phi} \quad (3)$$

where $s = \sqrt{\mu_x^2 + \mu_y^2}$ is the boresight displacement with μ_x and μ_y representing horizontal and vertical boresight values, respectively, S_0 is the fraction of collected power without pointing errors, ϕ is the ratio of normalized beam-width to the jitter, and $I_0(\cdot)$ denotes the modified Bessel function of the first kind with order zero.

We denote by $A_t = \frac{\alpha_t \mu_t}{\Omega^{\alpha_t \mu_t} \Gamma(\mu_t)}$, and $B_t = \frac{\mu_t}{\Omega^{\alpha_t \mu_t}}$. Denoting $\bar{\gamma}_r = \frac{P_r |H_r|^2}{\sigma_{w_r}^2}$ with P_r as the transmit power at the source for the RF transmission and $\bar{\gamma}_t = \frac{P_t |H_t|^2}{\sigma_{w_t}^2}$ with P_t as the transmit power at the relay for the THz transmission, we express the SNR of the RF link as $\gamma_r = \bar{\gamma}_r |h_f|^2$ and the SNR of the THz as $\gamma_t = \bar{\gamma}_t |h_f h_p|^2$. The end-to-end SNR AF relaying system is given by $\gamma = \frac{\bar{\gamma}_r \bar{\gamma}_t}{\bar{\gamma}_r + C}$ [13] where $C = P_t / \mathcal{G}^2 \sigma_{w_t}^2$. For the blind AF relaying, an arbitrary value of \mathcal{G} can be selected. However, in a semi-blind approach the fixed gain relaying factor \mathcal{G} can be obtained using statistics of received signal of the first hop $C = (\mathbb{E}_{\gamma_r} (1 + \gamma)^{-1})^{-1}$ [13], where \mathbb{E}_{γ_r} denotes the expectation operator over the random variable γ_r . Hence, the well-known PDF of end-to-end SNR γ of the fixed-

gain AF relaying system is given by

$$f_\gamma(z) = \int_0^\infty f_{\gamma_r}\left(\frac{z(x+C)}{x}\right) f_{\gamma_t}(x) \frac{x+C}{x} dx \quad (4)$$

III. PERFORMANCE ANALYSIS

In this section, we provide statistical results for the AF relaying by deriving analytical expressions of the PDF and CDF of the THz link. Using the derived statistical results, we analyze the outage probability, average BER, and ergodic capacity performance of mixed RF-THz system.

A. Density and Distribution Functions

In the following, we present the PDF and CDF of SNR for the THz link subjected to short-term fading and pointing errors. Using the limits of $|h_{ft}|$ and h_p in (2) and (3), respectively, the PDF of $|h_{fp}| = h_p |h_{ft}|$ can be represented as

$$f_{|h_{fp}|}(h) = \int_0^{S_0} \frac{1}{h_p} f_{h_f}\left(\frac{h}{h_p}\right) f_{|h_p|}(h_p) dh_p \quad (5)$$

Using (3) with the series expansion $I_0(x) = \sum_{k=0}^\infty \frac{\left(\frac{x}{2}\right)^{2k}}{(k!)^2}$ in (5) and utilizing the integral form of Meijer's G-function:

$$f_{h_{fp}}(h) = \frac{A_t \phi \exp\left(\frac{-s^2}{2\sigma^2}\right) h^{(\alpha_t \mu_t - 1)}}{A_0^\phi} \sum_{j=0}^\infty \frac{1}{(j!)^2} \left(\frac{s^2 w_{zeq}^2}{8\sigma^4}\right)^j \frac{1}{2\pi i} \int_{\mathcal{L}} \Gamma(0 - u_1) (B_t h^{\alpha_t})^u du I_1 \quad (6)$$

where $I_1 = \int_0^{S_0} h_p^{(\phi - \alpha_t \mu_t - 1)} h_p^{-\alpha_t u} \left(\ln \frac{S_0}{h_p}\right)^j dh_p$. Substituting $\ln \frac{S_0}{h_p} = t$, we obtain $I_1 = S_0^{(\phi - \alpha_t \mu_t + 1 - \alpha_t u)} \Gamma(j + 1) \left(\frac{\Gamma(1 + \phi - \alpha_t \mu_t - \alpha u)}{\Gamma(\phi - \alpha_t \mu_t - \alpha u)}\right)^{-(j+1)}$. Further, using I_1 in (6) and applying the definition of Fox's H-function [26] with a transformation of the random variable $f_{\gamma_t}(\gamma) = \frac{1}{2\sqrt{\gamma \bar{\gamma}_t}} f_{h_{fp}}\left(\sqrt{\frac{\gamma}{\bar{\gamma}_t}}\right)$ we get the PDF

$$f_{\gamma_t}(\gamma) = \frac{A_t \phi \exp\left(\frac{-s^2}{2\sigma^2}\right) S_0^{(-\alpha_t \mu_t + 1)} \gamma^{\frac{\alpha_t \mu_t}{2} - 1}}{2\bar{\gamma}_t^{\frac{\alpha_t \mu_t}{2}}} \sum_{j=0}^\infty \frac{1}{j!} \left(\frac{s^2 w_{zeq}^2}{8\sigma^4}\right)^j H_{j+1, k+2}^{k+2, 0} \left[\frac{B_t \gamma^{\frac{\alpha_t}{2}}}{S_0^{\alpha_t} \bar{\gamma}_t^{\frac{\alpha_t}{2}}} \middle| (1 + \phi - \alpha_t \mu_t, 1)^{j+1}, (0, 1), (\phi - \alpha_t \mu_t, 1)^{j+1} \right] \quad (7)$$

We use the PDF (7) in $\int_0^\gamma f_{\gamma_t}(z) dz$ and simplify the integral using the Mellin Barnes integral representation of the Fox's H-function to get the CDF:

$$F_{\gamma_t}(x) = \frac{A_t \phi \exp\left(\frac{-s^2}{2\sigma^2}\right) S_0^{(-\alpha_t \mu_t + 1)} \gamma^{\frac{\alpha_t \mu_t}{2}}}{2\bar{\gamma}_t^{\frac{\alpha_t \mu_t}{2}}} \sum_{j=0}^\infty \frac{1}{j!} \left(\frac{s^2 w_{zeq}^2}{8\sigma^4}\right)^j H_{j+1, j+3}^{k+2, 1} \left[\frac{B_t \gamma^{\frac{\alpha_t}{2}}}{S_0^{\alpha_t} \bar{\gamma}_t^{\frac{\alpha_t}{2}}} \middle| \left(1 - \frac{\alpha_t \mu_t}{2}, \frac{\alpha_t}{2}\right), (1 + \phi - \alpha_t \mu_t, 1)^{j+1}, (0, 1), (\phi - \alpha_t \mu_t, 1)^{j+1}, \left(-\frac{\alpha_t \mu_t}{2}, \frac{\alpha_t}{2}\right) \right] \quad (8)$$

Note that the use of Meijer's G and Fox's H functions is common in the research fraternity and can be efficiently evaluated using built-in functions available in computational software such as MATLAB and MATHEMATICA. We capitalize results of (7) and (8) to present the PDF of SNR for the AF relaying in terms of bivariate Fox's H function.

Representing exponential and hypergeometric functions of (1) into Meijer's G-function with a transformation of random variable $\gamma_r = \bar{\gamma}_r |h_f|^2$, we get

$$f_{\gamma_r}(x) = \frac{m_r^{m_r} \alpha_r}{2c_r^{\mu_r} \Gamma(\mu_r)(\mu_r \kappa_r + m_r)_r m_r \bar{x}} \left(\frac{x}{\bar{\gamma}_r}\right)^{\frac{\alpha_r \mu_r}{2} - 1} G_{0,1}^{1,0} \left(\frac{x}{c \bar{\gamma}_r^{\frac{\alpha_r}{2}}} \middle| -\right) \frac{\Gamma(\mu_r)}{\Gamma(m_r)} G_{1,2}^{1,1} \left(\frac{-\mu_r \kappa_r x^{\frac{\alpha_r}{2}}}{c(\mu_r \kappa_r + m_r) \bar{\gamma}_r^{\frac{\alpha_r}{2}}} \middle| \frac{1 - m_r}{0}, 1 - \mu_r\right) \quad (9)$$

¹Notations: Subscripts $(\cdot)_R$, $(\cdot)_D$, $(\cdot)_r$, and $(\cdot)_t$ denote the relay, destination, the first link RF, and second link THz, respectively. $G_{p,q}^{m,n}(\cdot)$ and $H_{p,q}^{m,n}(\cdot)$ denotes Meijer's G and Fox's H-functions, respectively.

Substituting (7) and (9) in (4) and utilizing the integral representation of Fox's H-function with a change in the order of integration:

$$f_\gamma(\gamma) = \frac{m_r^{m_r} \alpha_r \gamma^{\frac{\alpha_r \mu_r}{2} - 1}}{2c^{\mu_r} (\mu_r \kappa_r + m_r)^{m_r} \bar{\gamma}_r \Gamma(m_r) \bar{\gamma}_r^{\frac{\alpha_r \mu_r}{2} - 1}} \frac{A_t \phi \exp\left(\frac{-s^2}{2\sigma^2}\right) S_0^{(-\alpha_t \mu_t + 1)}}{2\bar{\gamma}_t^{\frac{\alpha_t \mu_t}{2}}} \sum_{j=0}^{\infty} \frac{\Gamma(j+1)}{(j!)^2} \left(\frac{s^2 w_{z_{\text{eq}}}^2}{8\sigma^4}\right)^j \frac{1}{2\pi i} \int_{\mathcal{L}_1} \frac{\Gamma(0-u_1) \Gamma(0-u_1) \Gamma(m_r+u_1)}{\Gamma(\mu_r+u_1)} \left(\frac{-\mu_r \kappa_r \gamma^{\alpha_r}}{c^2 (\mu_r \kappa_r + m_r) \bar{\gamma}_r^{\alpha_r}}\right)^{u_1} du_1 \frac{1}{2\pi i} \int_{\mathcal{L}_2} \frac{\Gamma(0-u_2) \Gamma(\phi - \alpha_t \mu_t - \alpha_t u_2)^{(j+1)}}{\Gamma(1+\phi - \alpha_t \mu_t - \alpha_t u_2)^{(j+1)}} \left(\frac{B_t C \frac{\alpha_t}{2}}{S_0^{\alpha_t} \bar{\gamma}_t^{\frac{\alpha_t}{2}}}\right)^{u_2} du_2 I_2 \quad (10)$$

where \mathcal{L}_1 and \mathcal{L}_2 denote the contour integrals. We use [27, (3.194/3)] and [27, (8.384/1)] to solve the inner integral I_2 in terms of the compatible Gamma function:

$$\int_0^\infty \left(\frac{\gamma+C}{x}\right)^{\left(\frac{\alpha_r \mu_r}{2} + \alpha_r u_1\right)} \gamma^{\frac{\alpha_t \mu_t + \alpha_t u_2}{2} - 1} d\gamma = \frac{C^{\frac{\alpha_t \mu_t + \alpha_t u_2}{2}} \Gamma\left(\frac{-\alpha_t \mu_t - \alpha_t u_2}{2}\right) \Gamma\left(\frac{-\alpha_r \mu_r - 2\alpha_r u_1 + \alpha_t \mu_t + \alpha_t u_2}{2}\right)}{\Gamma\left(\frac{-\alpha_r \mu_r - 2\alpha_r u_1}{2}\right)} \quad (11)$$

Finally, we substitute (11) in (10), and to apply the definition of Fox's H function [28, (1.1)], we use $u_1 \rightarrow -u_1$ in (10) to get the PDF for fixed-gain relaying:

$$f_\gamma(\gamma) = \frac{m_r^{m_r} \alpha_r C^{\frac{\alpha_t \mu_t}{2}} A_t \phi \exp\left(\frac{-s^2}{2\sigma^2}\right) S_0^{(-\alpha_t \mu_t + 1)} \gamma^{\frac{\alpha_r \mu_r}{2} - 1}}{4c^{\mu_r} (\mu_r \kappa_r + m_r)^{m_r} \Gamma(m_r) \bar{\gamma}_r^{\frac{\alpha_r \mu_r}{2}} \bar{\gamma}_t^{\frac{\alpha_t \mu_t}{2}}} \sum_{j=0}^{\infty} \frac{1}{j!} \left(\frac{s^2 w_{z_{\text{eq}}}^2}{8\sigma^4}\right)^j H_{1,0;1,1;2,j+3,0}^{1,0;3,2;j+1,j+3} \left[\frac{c^2 (\mu_r \kappa_r + m_r) \bar{\gamma}_r^{\alpha_r}}{-\mu_r \kappa_r \gamma^{\alpha_r}}; \frac{B_t C \frac{\alpha_t}{2}}{S_0^{\alpha_t} \bar{\gamma}_t^{\frac{\alpha_t}{2}}} \left| \begin{matrix} V_1 \\ V_2 \end{matrix} \right. \right] \quad (12)$$

where $V_1 = \left\{ \left(1 - \frac{\alpha_t \mu_t - \alpha_r \mu_r}{2}; \alpha_r, \frac{\alpha_t}{2}\right); \left\{ (1, 1), (1, 1), (\mu_r, 1) \right\}; \left\{ \left(1 + \phi - \alpha_t \mu_t, \alpha_t\right)^{j+1} \right\} \right\}$, and $V_2 = \left\{ -\right\}; \left\{ (m_r, 1), \left(1 + \frac{\alpha_r \mu_r}{2}, \alpha_r\right); \left\{ (0, 1), \left(\phi - \alpha_t \mu_t, \alpha_t\right)^{j+1}, \left(-\frac{\alpha_t \mu_t}{2}, \frac{\alpha_t}{2}\right) \right\} \right\}$.

B. Outage Probability

Outage probability is defined as the probability of SNR being less than a threshold value γ_{th} i.e., $P_{\text{out}} = P(\gamma < \gamma_{th}) = F_\gamma(\gamma_{th})$. Thus, using (12) in $F_\gamma(\gamma) = \int_0^\gamma f_\gamma(z) dz$, and applying the definition of Fox's H function with the following inner integral

$$\int_0^\gamma z^{\frac{\alpha_r \mu_r}{2} - 1} z^{-\alpha_r u_1} dz = \frac{z^{\frac{\alpha_r \mu_r}{2}} z^{-\alpha_r u_1} \Gamma\left(\frac{\alpha_r \mu_r - 2\alpha_r u_1}{2}\right)}{\Gamma\left(1 + \frac{\alpha_r \mu_r - 2\alpha_r u_1}{2}\right)} \quad (13)$$

we get the CDF as

$$F_\gamma(\gamma) = \frac{m_r^{m_r} \alpha_r C^{\frac{\alpha_t \mu_t}{2}} A_t \phi \exp\left(\frac{-s^2}{2\sigma^2}\right) S_0^{(-\alpha_t \mu_t + 1)} \gamma^{\frac{\alpha_r \mu_r}{2}}}{4c^{\mu_r} (\mu_r \kappa_r + m_r)^{m_r} \Gamma(m_r) \bar{\gamma}_r^{\frac{\alpha_r \mu_r}{2}} \bar{\gamma}_t^{\frac{\alpha_t \mu_t}{2}}} \sum_{j=0}^{\infty} \frac{1}{j!} \left(\frac{s^2 w_{z_{\text{eq}}}^2}{8\sigma^4}\right)^j H_{0,1;2,2;j+3,0}^{1,0;4,3;j+1,j+3} \left[\frac{c^2 (\mu_r \kappa_r + m_r) \bar{\gamma}_r^{\alpha_r}}{-\mu_r \kappa_r \gamma^{\alpha_r}}; \frac{B_t C \frac{\alpha_t}{2}}{S_0^{\alpha_t} \bar{\gamma}_t^{\frac{\alpha_t}{2}}} \left| \begin{matrix} Q_1 \\ Q_2 \end{matrix} \right. \right] \quad (14)$$

where $Q_1 = \left\{ \left(1 - \frac{\alpha_t \mu_t - \alpha_r \mu_r}{2}; \alpha_r, \frac{\alpha_t}{2}\right); \left\{ (1, 1), (1, 1), (\mu_r, 1), \left(1 + \frac{\alpha_r \mu_r}{2}, \alpha_r\right); \left\{ \left(1 + \phi - \alpha_t \mu_t, \alpha_t\right)^{j+1} \right\} \right\}$, and $Q_2 = \left\{ -\right\}; \left\{ (m_r, 1), \left(\frac{\alpha_r \mu_r}{2}, \alpha_r\right), \left(1 + \frac{\alpha_r \mu_r}{2}, \alpha_r\right); \left\{ (0, 1), \left(\phi - \alpha_t \mu_t, \alpha_t\right)^{j+1}, \left(-\frac{\alpha_t \mu_t}{2}, \frac{\alpha_t}{2}\right) \right\} \right\}$.

To derive the asymptotic outage probability in the high SNR regime, we use [26, Theorems 1.7, 1.11] and compute residues of (14) for both contours \mathcal{L}_1 and \mathcal{L}_2 at poles $u_1 = 0, 0, \frac{-\alpha_r \mu_r + \alpha_t \mu_t + \alpha_t u_2}{2\alpha_r}$ and $s_2 = 0, -\mu_t$, and $\frac{\phi - \alpha_t \mu_t}{\alpha_t}$. Simplifying the derived residues, we present the asymptotic expression in

(15). It should be emphasized that the consideration of all the poles may result into our asymptotic analysis close to the exact for a wide range of SNR. Further, it can be easily seen from (15) that the outage diversity order of the system is $\min\left\{\frac{\alpha_r \mu_r}{2}, \frac{\alpha_t \mu_t}{2}, \frac{\phi}{2}\right\}$. Note that the derived diversity order for the THz-RF can be confirmed individually with previous results on α - μ fading [9] and α -KMS [23].

C. Average BER

The average BER of a communication system is given as:

$$\overline{BER} = \frac{q^p}{2\Gamma(p)} \int_0^\infty \gamma^{p-1} e^{-q\gamma} F_\gamma(\gamma) d\gamma \quad (16)$$

where p and q are modulation-dependent constants. Using CDF of (14) in (16), the average BER can be expressed as

$$\overline{BER} = \frac{m_r^{m_r} \alpha_r C^{\frac{\alpha_t \mu_t}{2}} A_t \phi \exp\left(\frac{-s^2}{2\sigma^2}\right) S_0^{(-\alpha_t \mu_t + 1)} q^p}{8c^{\mu_r} (\mu_r \kappa_r + m_r)^{m_r} \Gamma(m_r) \Gamma(p) \bar{\gamma}_r^{\frac{\alpha_r \mu_r}{2}} \bar{\gamma}_t^{\frac{\alpha_t \mu_t}{2}}} \sum_{j=0}^{\infty} \frac{\Gamma(j+1)}{(j!)^2} \left(\frac{s^2 w_{z_{\text{eq}}}^2}{8\sigma^4}\right)^j \frac{1}{2\pi i} \int_{\mathcal{L}_1} \frac{\Gamma(0+u_1) \Gamma(0+u_1) \Gamma(m_r-u_1)}{\Gamma(\mu_r-u_1)} \left(\frac{c^2 (\mu_r \kappa_r + m_r) \bar{\gamma}_r^{\alpha_r}}{-\mu_r \kappa_r}\right)^{u_1} du_1 \frac{1}{2\pi i} \int_{\mathcal{L}_2} \frac{\Gamma(0-u_2) \Gamma(\phi - \alpha_t \mu_t - \alpha_t u_2)^{(j+1)}}{\Gamma(1+\phi - \alpha_t \mu_t - \alpha_t u_2)^{(j+1)}} \left(\frac{B_t C \frac{\alpha_t}{2}}{S_0^{\alpha_t} \bar{\gamma}_t^{\frac{\alpha_t}{2}}}\right)^{u_2} du_2 \frac{\Gamma\left(\frac{-\alpha_t \mu_t - \alpha_t u_2}{2}\right) \Gamma\left(\frac{-\alpha_r \mu_r + \alpha_t \mu_t + 2\alpha_r u_1 + \alpha_t u_2}{2}\right) \Gamma\left(\frac{\alpha_r \mu_r - 2\alpha_r u_1}{2}\right)}{\Gamma\left(\frac{-\alpha_r \mu_r + 2\alpha_r u_1}{2}\right) \Gamma\left(1 + \frac{\alpha_r \mu_r - 2\alpha_r u_1}{2}\right)} \int_0^\infty \gamma^{p-1} e^{-q\gamma} \gamma^{\frac{\alpha_r \mu_r - 2\alpha_r u_1}{2}} d\gamma \quad (17)$$

Using the solution of inner integral $\int_0^\infty \gamma^{p-1} e^{-q\gamma} \gamma^{\frac{\alpha_r \mu_r - 2\alpha_r u_1}{2}} d\gamma$ [27, (3.381/4)] in terms of Gamma function, and applying the definition of Fox's H function [28, (1.1)], we get

$$\overline{BER} = \frac{m_r^{m_r} \alpha_r C^{\frac{\alpha_t \mu_t}{2}} A_t \phi \exp\left(\frac{-s^2}{2\sigma^2}\right) S_0^{(-\alpha_t \mu_t + 1)} q^{\frac{-\alpha_r \mu_r}{2}}}{8c^{\mu_r} (\mu_r \kappa_r + m_r)^{m_r} \Gamma(m_r) \Gamma(p) \bar{\gamma}_r^{\frac{\alpha_r \mu_r}{2}} \bar{\gamma}_t^{\frac{\alpha_t \mu_t}{2}}} \sum_{j=0}^{\infty} \frac{1}{j!} \left(\frac{s^2 w_{z_{\text{eq}}}^2}{8\sigma^4}\right)^j H_{0,1;3,2;j+3,0}^{1,0;4,4;j+1,j+3} \left[\frac{c^2 (\mu_r \kappa_r + m_r) \bar{\gamma}_r^{\alpha_r} q^{\alpha_r}}{-\mu_r \kappa_r}; \frac{B_t C \frac{\alpha_t}{2}}{S_0^{\alpha_t} \bar{\gamma}_t^{\frac{\alpha_t}{2}}} \left| \begin{matrix} U_1 \\ U_2 \end{matrix} \right. \right] \quad (18)$$

where $U_1 = \left\{ \left(1 - \frac{\alpha_t \mu_t - \alpha_r \mu_r}{2}; \alpha_r, \frac{\alpha_t}{2}\right); \left\{ (1, 1), (1, 1), (\mu_r, 1), \left(1 + \frac{\alpha_r \mu_r}{2}, \alpha_r\right); \left\{ \left(1 + \phi - \alpha_t \mu_t, \alpha_t\right)^{j+1} \right\} \right\}$, and $U_2 = \left\{ -\right\}; \left\{ (m_r, 1), \left(\frac{\alpha_r \mu_r}{2}, \alpha_r\right), \left(p + \frac{\alpha_r \mu_r}{2}, \alpha_r\right), \left(1 + \frac{\alpha_r \mu_r}{2}, \alpha_r\right); \left\{ (0, 1), \left(\phi - \alpha_t \mu_t, \alpha_t\right)^{j+1}, \left(-\frac{\alpha_t \mu_t}{2}, \frac{\alpha_t}{2}\right) \right\} \right\}$.

Similar to the asymptotic expression of the outage probability, we derive the average BER at the high SNR \overline{BER}^∞ in terms of simpler Gamma function, as given in (15), and the corresponding diversity order as $\min\left\{\frac{\alpha_r \mu_r}{2}, \frac{\alpha_t \mu_t}{2}, \frac{\phi}{2}\right\}$.

D. Ergodic Capacity

The ergodic capacity is defined as

$$\bar{C} = \int_0^\infty \log_2(1 + \gamma) f_\gamma(\gamma) d\gamma \quad (19)$$

Thus, substituting the PDF (12) in (19), we apply the definition of Fox's H resulting into the inner integral as [27, (4.293.3)]

$$\int_0^\infty \log_2(1 + \gamma) \gamma^{\frac{\alpha_r \mu_r}{2} - 1} \gamma^{-\alpha_r u_1} d\gamma = \frac{\pi C s c \left(\frac{\alpha_r \mu_r - 2\alpha_r u_1}{2}\right)}{\log(2) \frac{\alpha_r \mu_r - 2\alpha_r u_1}{2}} \quad (20)$$

$$\Psi^\infty = G_0 \left[G_1 \left(\frac{-\mu_r \kappa_r \gamma^{\alpha_r}}{c^2 (\mu_r \kappa_r + m_r)} \right)^{\frac{\alpha_t \mu_t - \mu_r}{2\alpha_r} - \frac{\mu_r}{2}} \bar{\gamma}_r^{-\frac{\alpha_t \mu_t}{2}} + G_2 \left(\frac{B_t C \frac{\alpha_t}{2}}{S_0^{\alpha_t} \bar{\gamma}_t^{\frac{\alpha_t}{2}}} \right)^{\frac{\phi - \alpha_t \mu_t}{\alpha_t}} \left(\frac{-\mu_r \kappa_r \gamma^{\alpha_r}}{c^2 (\mu_r \kappa_r + m_r)} \right)^{\frac{\phi}{2\alpha_r} - \frac{\mu_r}{2}} \bar{\gamma}_r^{-\frac{\phi}{2}} + G_3 \bar{\gamma}_r^{-\frac{\alpha_r \mu_r}{2}} \right] \quad (15)$$

where $G_0 = \frac{m_r^{m_r} \alpha_r A_t \phi \exp\left(-\frac{s^2}{2\sigma^2}\right) S_0^{(-\alpha_t \mu_t + 1) \phi}}{4c^{\mu_r} (\mu_r \kappa_r + m_r)^{m_r} \Gamma(m_r)} \sum_{j=0}^{\infty} \frac{1}{j!} \left(\frac{s^2 w_{zeq}^2}{8\sigma^4} \right)^j$, $G_1 = \frac{\Gamma\left(\frac{\alpha_r \mu_r - \alpha_t \mu_t}{2\alpha_r}\right) \Gamma\left(\frac{\alpha_r \mu_r - \alpha_t \mu_t}{2\alpha_r}\right) \Gamma(m_r + \frac{-\alpha_r \mu_r + \alpha_t \mu_t}{2\alpha_r}) \Gamma\left(\frac{-\alpha_t \mu_t}{2}\right) C^{\frac{\alpha_t \mu_t}{2}} \zeta_1}{\Gamma(\mu_r + \frac{-\alpha_r \mu_r + \alpha_t \mu_t}{2\alpha_r}) \Gamma(-\alpha_t \mu_t) \alpha_t \mu_t (\phi - \alpha_t \mu_t)^{(j+1)} \bar{\gamma}_t^{\frac{\alpha_t \mu_t}{2}}}$

$$G_2 = \frac{\Gamma\left(\frac{\alpha_r \mu_r - \phi}{2\alpha_r}\right) \Gamma\left(\frac{\alpha_r \mu_r - \phi}{2\alpha_r}\right) \Gamma(m_r + \frac{-\alpha_r \mu_r + \phi}{2\alpha_r}) \Gamma\left(\frac{\alpha_t \mu_t - \phi}{2}\right) \Gamma\left(\frac{-\phi}{2}\right) C^{\frac{\alpha_t \mu_t}{2}} \zeta_2}{\Gamma(\mu_r + \frac{-\alpha_r \mu_r + \phi}{2\alpha_r}) \Gamma(-\phi) \phi \bar{\gamma}_t^{\frac{\alpha_t \mu_t}{2}}}$$

$$G_3 = \left(\frac{2C \frac{\alpha_t \mu_t}{2} \zeta_3}{\bar{\gamma}_t^{\frac{\alpha_t \mu_t}{2}}} \right) \left(\frac{\Gamma\left(\frac{-\alpha_r \mu_r + \alpha_t \mu_t}{2}\right) \Gamma(m_r) \Gamma\left(\frac{-\alpha_t \mu_t}{2}\right)}{\Gamma(\mu_r) \Gamma\left(\frac{-\alpha_r \mu_r}{2}\right) \frac{\alpha_r \mu_r}{2} (\phi - \alpha_t \mu_t)^{(j+1)}} + \frac{\Gamma(m_r) \Gamma(\mu_t)}{\Gamma(\mu_r) \Gamma(\mu_t)} \left(\frac{B_t C \frac{\alpha_t}{2}}{S_0^{\alpha_t} \bar{\gamma}_t^{\frac{\alpha_t}{2}}} \right)^{-\mu_t} + \frac{\Gamma\left(\frac{-\alpha_r \mu_r + \phi}{2}\right) \Gamma(m_r) \Gamma\left(\frac{\alpha_t \mu_t - \phi}{2}\right) \Gamma\left(\frac{-\phi}{2}\right) \left(\frac{B_t C \frac{\alpha_t}{2}}{S_0^{\alpha_t} \bar{\gamma}_t^{\frac{\alpha_t}{2}}} \right)^{\frac{\phi - \alpha_t \mu_t}{\alpha_t}} + \frac{\Gamma\left(\frac{\mu_r}{2}\right) \Gamma(m_r + \frac{-\mu_r}{2}) \Gamma(\mu_t) C^{\frac{\alpha_t \mu_t}{2}} \zeta_4}{(\phi)^{(j+1)} \bar{\gamma}_t^{\frac{\alpha_t \mu_t}{2}}} \left(\frac{-\mu_r \kappa_r \gamma^{\alpha_r}}{c^2 (\mu_r \kappa_r + m_r)} \right)^{-\frac{\mu_r}{2}} \left(\frac{B_t C \frac{\alpha_t}{2}}{S_0^{\alpha_t} \bar{\gamma}_t^{\frac{\alpha_t}{2}}} \right)^{-\mu_t} \right); \Psi^\infty = P_{\text{out}}^\infty \text{ when } \varphi = \gamma_{\text{th}}^{\frac{\alpha_t \mu_t}{2}} \text{ and } \zeta_1 = \zeta_2 = \zeta_3 = \zeta_4 = 1; \Psi^\infty = \overline{BER}^\infty \text{ when } \varphi = \frac{q - (\frac{\alpha_r \mu_r}{2} + p)}{2\Gamma(p)}, \zeta_1 = \Gamma(p + \frac{\alpha_r \mu_r}{2}), \zeta_2 = \Gamma(p), \zeta_3 = \Gamma(p + \frac{\alpha_t \mu_t}{2}), \text{ and } \zeta_4 = \Gamma(p + \frac{\phi}{2}).$$

Finally, we apply the identity $\pi Csc(\pi a) = \Gamma(a)\Gamma(1-a)$ in (20) along with the Fox's H function [28, (1.1)] to get the ergodic capacity:

$$\bar{C} = \frac{m_r^{m_r} \alpha_r C^{\frac{\alpha_t \mu_t}{2}} A_t \phi \exp\left(-\frac{s^2}{2\sigma^2}\right) S_0^{(-\alpha_t \mu_t + 1)}}{\log(2) 4c^{\mu_r} (\mu_r \kappa_r + m_r)^{m_r} \Gamma(m_r) \bar{\gamma}_r} \sum_{j=0}^{\infty} \frac{1}{j!} \left(\frac{s^2 w_{zeq}^2}{8\sigma^4} \right)^j H_{1,0:4,2;j+3,0}^{0,1:4,2;j+3,0} \left[\frac{c^2 (\mu_r \kappa_r + m_r) \bar{\gamma}_r^{\alpha_r}}{-\mu_r \kappa_r}; \frac{B_t C \frac{\alpha_t}{2}}{S_0^{\alpha_t} \bar{\gamma}_t^{\frac{\alpha_t}{2}}} \middle| \begin{matrix} D_1 \\ D_2 \end{matrix} \right] \quad (21)$$

where $D_1 = \left\{ \left(1 - \frac{\alpha_t \mu_t - \alpha_r \mu_r}{2}, \alpha_r, \frac{\alpha_t}{2} \right); \left(1, 1 \right), \left(1, 1 \right), \left(\mu_r, 1 \right), \left(1 + \frac{\alpha_r \mu_r}{2}, \alpha_r \right); \left\{ \left(1 + \phi - \alpha_t \mu_t, \alpha_t \right)^{j+1} \right\} \right\}$, and $D_2 = \left\{ - \right\}; \left\{ \left(m_r, 1 \right), \left(\frac{\alpha_r \mu_r}{2}, \alpha_r \right), \left(\frac{\alpha_r \mu_r}{2}, \alpha_r \right), \left(1 - \frac{\alpha_r \mu_r}{2}, \alpha_r \right), \left(1 + \frac{\alpha_r \mu_r}{2}, \alpha_r \right); \left\{ \left(0, 1 \right), \left(\phi - \alpha_t \mu_t, \alpha_t \right)^{j+1}, \left(-\frac{\alpha_t \mu_t}{2}, \frac{\alpha_t}{2} \right) \right\} \right\}$.

IV. SIMULATION RESULTS AND DISCUSSIONS

We demonstrate the performance of the considered RF-THz wireless system and validate our derived analytical results using numerical analysis and Monte-Carlo simulations. To evaluate analytical expressions in (14), (18), and (21), we use MATLAB implementation of bivariate Fox's H function [29], and take 10 terms for the convergence of infinite series. The bivariate Fox's H-function requires the computation of two contour integrals involving the ratio of the product of Gamma functions. We also compare the proposed method with the existing DF relaying for the RF-THz system with zero-boresight pointing errors [8], [9]. To compute the path gain of the RF link with antenna gain $G_r = 26\text{dBi}$, we use path loss $L_r(\text{dB}) = 32.4 + 17.3 \log_{10}(d_2) + 20 \log_{10}(10^{-9} f_r)$ [9], where d_r is taken in the range of 50m to 200m, and $f_r = 6\text{GHz}$ is the carrier frequency of the RF. We compute path gain of THz link as $H_t = \frac{cG_t}{4\pi f_t d_t} \exp(-\frac{1}{2} k d_t)$, where $G_t = 55\text{dBi}$, $k = 2.8 \times 10^{-4}$ is the absorption coefficient [8], c is the speed of light, $f_t = 0.275\text{ THz}$, and $d_t = 50\text{m}$. We use [25] to compute the parameters of pointing errors with 10cm antenna aperture radius. A noise floor of -170dBm/Hz is taken for both THz and RF systems with 10GHz and 20MHz as the signal bandwidth for THz and RF transmissions, respectively [30].

First, we illustrate the impact of multipath clustering on the THz link (i.e., μ_t) and the effect of non-zero boresight and jitter of pointing errors (i.e., σ_s and s) by plotting the outage probability versus average SNR of the RF link $\bar{\gamma}_r$, as depicted in Fig. 1(a). We consider α -KMS parameters as $\{\alpha_r = 1.8, \mu_r = 2, \kappa_r = 4, m_r = 2\}$. Fig. 1(a) shows that the outage probability improves with an increase in μ_t since

the multipath clustering enhances channel conditions. Further, the figure shows that the effect of jitter is lesser at a higher $\mu_t = 2.4$ and low RF average SNR but incurs a penalty of almost 3 dB if σ_s is increased from 5 cm to 15cm at a lower $\mu_t = 1.2$ and outage probability 10^{-3} . It can also be seen from Fig. 1(a) that the non-zero values of boresight incurs higher pointing errors degrading marginally the outage probability as compared to the zero-boresight. The figure also shows that fixed-gain AF relaying performs close to the DF without expensive decoding procedure and continuous monitoring of CSI in most of the scenarios.

Next, we depict the impact of non-linearity of the THz fading and shadowing effect of the RF link considering non-zero boresight parameter $s = 14.14\text{ m}$ and jitter $\sigma_s = 5\text{ cm}$ with $\mu_t = 1.2$ on the average BER performance in Fig. 1(b). The figure shows a significant impact of the non-linearity factor α_t on the BER performance of the considered system. As such, the BER improves 10 fold at a average SNR of 40 dB when the parameter α_t increases from 1.4 to 2.6 to get an average BER of 2×10^{-5} . It can also be observed from the figure that the average BER performance degrades when the shadowing parameter increases from $m_r = 6$ (less shadowing) to $m_r = 1$ (severe shadowing). Further, with an increase in the parameter $\kappa_r = 2$ to $\kappa_r = 8$ at the given shadowing value, the average BER decreases marginally.

We demonstrate the impact of various parameters on the outage probability and average BER for a better insight into system performance. Note that $\phi = 37$ when $\sigma_s = 5$ and cm) and $\phi = 4.1184$ when $\sigma_s = 15\text{ cm}$ [25]. When $\mu_t = 1.2$, the outage diversity order is 0.9 since $\alpha_t \mu_t = 1.8$ is the minimum of $\alpha_r \mu_r = 3.6$ and $\phi = 4.1184$. Similarly, the diversity order becomes 1.8 when $\mu_t = 2.4$. Fig. 1(a) shows that there is a change in the slope of plots corresponding to $\mu_t = 1.2$ and $\mu_t = 2.4$, but there is no change in the slope when pointing error parameters are changed. Thus, the diversity order analysis provides a design consideration to use high beam-width to compensate for the effect of pointing errors. Similar to the outage probability, the BER diversity order depends on the fading parameters of the THz link (i.e., $\alpha_t \mu_t = \{1.68, 3.12\}$) and becomes independent of pointing errors since $\phi (= 37) > \mu_t \alpha_t$ and $\alpha_r \mu_r (= 3.6) > \alpha_t \mu_t$. The plots confirm our analysis on the diversity order since there is a change in the slope of the plots in Fig 1(b) for different values of α_t and the slope does not change with the α -KMS parameters κ_r and m_r . Thus, the proposed analysis provides an insight into the deployment scenarios for the mixed RF-THz relaying considering various system and channel configurations.

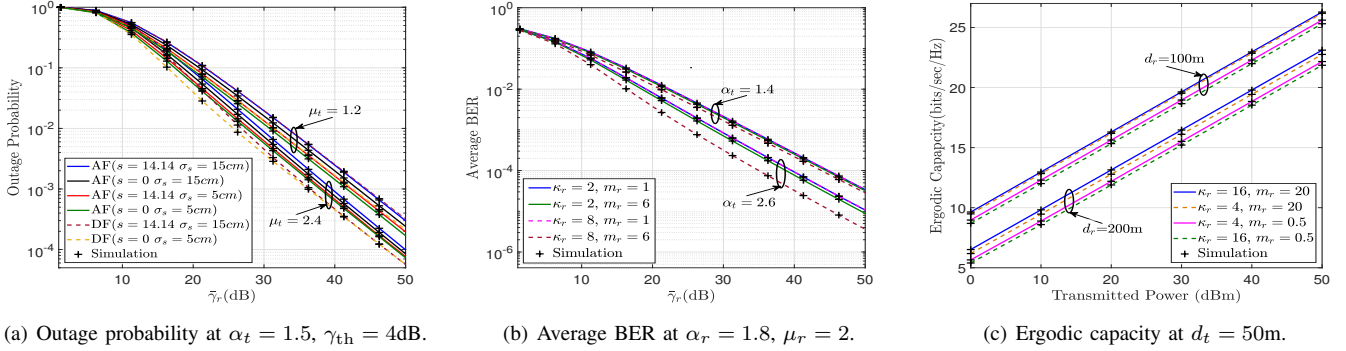


Fig. 1. Performance of fixed-gain relay-assisted RF-THz wireless link over mixed fading with non-zero pointing errors.

Finally, Fig 1(c) presents the ergodic capacity performance for various RF link distance $d_r = 100$ m and $d_r = 200$ m at a fixed THz link distance with $\alpha_t = 2$, $\mu_t = 2.2$, $\alpha_r = 1.8$, $\mu_r = 2$, and $\sigma_s = 10.6$ cm. This can be a typical situation for front-hauling with THz transmissions and broadband mobile access using the RF technology. Fig 1(c) shows that the ergodic capacity decreases with an increase in the RF link distance by 3 bits/sec/Hz when d_r is increased from 100 m to 200 m. Still, the ergodic capacity is significantly higher at 13 bits/sec/Hz at a transmit power of 20 dBm at $d_r = 200$ m. The figure also shows the effect of shadowing m_r and parameter κ_r (which is ratio of the total power of the dominant components and the total power of the scattered waves). It can be seen that the performance degrades with an increase in the shadowing effect (i.e., when m_r decreases from 20 to 0.5) and a marginal change in the ergodic capacity with the parameter κ_r .

We envision that the proposed RF-THz can be a viable alternative for the convergence of access networks and front-haul/backhaul links over wireless technology. Consideration of co-channel interference and hardware impairment in the THz transmission link are a few possible directions for future works.

REFERENCES

- [1] H. Elayan *et al.*, "Terahertz band: The last piece of RF spectrum puzzle for communication systems," *IEEE Open J. of the Commun. Soc.*, vol. 1, pp. 1–32, 2020.
- [2] S. Koenig *et al.*, "Wireless sub-THz communication system with high data rate," *Nature Photon.*, vol. 7, p. 977–981, 2013.
- [3] J. Kokkonen *et al.*, "Impact of beam misalignment on THz wireless systems," *Nano Commun. Netw.*, vol. 24, p. 100302, 2020.
- [4] Q. Xia and J. M. Jornet, "Cross-layer analysis of optimal relaying strategies for Terahertz-band communication networks," in *2017 IEEE 13th Int. Conf. on Wireless and Mobile Comput., Netw. and Commun. (WiMob)*, 2017, pp. 1–8.
- [5] G. Stratidakis *et al.*, "Relay-based blockage and antenna misalignment mitigation in THz wireless communications," in *2020 2nd 6G Wireless Summit (6G SUMMIT)*, 2020, pp. 1–4.
- [6] A. A. Boulogeorgos and A. Alexiou, "Outage probability analysis of THz relaying systems," in *2020 IEEE 31st Annu. Int. Symp. on Personal, Indoor and Mobile Radio Commun.*, 2020, pp. 1–7.
- [7] C. Huang *et al.*, "Multi-hop RIS-empowered Terahertz communications: A DRL-based hybrid beamforming design," *IEEE J. Sel. Areas Commun.*, vol. 39, no. 6, pp. 1663–1677, 2021.
- [8] A. A. Boulogeorgos and A. Alexiou, "Error analysis of mixed THz-RF wireless systems," *IEEE Commun. Lett.*, vol. 24, no. 2, pp. 277–281, 2020.
- [9] P. Bhardwaj and S. M. Zafaruddin, "Performance of dual-hop relaying for THz-RF wireless link over asymmetrical α - μ fading," *IEEE Trans. on Veh. Technol.*, vol. 70, no. 10, pp. 10031–10047, 2021.
- [10] Z. Rong *et al.*, "Relay-assisted nanoscale communication in the THz band," *Micro Nano Lett.*, vol. 12, no. 6, pp. 373–376, 2017.
- [11] Q. H. Abbasi *et al.*, "Cooperative In-Vivo nano-network communication at Terahertz frequencies," *IEEE Access*, vol. 5, pp. 8642–8647, 2017.
- [12] T. Mir *et al.*, "Hybrid precoding design for two-way relay-assisted Terahertz massive MIMO systems," *IEEE Access*, vol. 8, pp. 222 660–222 671, 2020.
- [13] M. Hasna and M.-S. Alouini, "A performance study of dual-hop transmissions with fixed gain relays," *IEEE Trans. Wireless Commun.*, vol. 3, no. 6, pp. 1963–1968, 2004.
- [14] S. Li and L. Yang, "Performance analysis of dual-hop THz transmission systems over α - μ fading channels with pointing errors," ArXiv: 2107.13166, July 2021.
- [15] S. H. Alvi *et al.*, "Performance analysis of dual-hop AF relaying over α - μ fading channels," *AEU - Int. J. of Electron. and Commun.*, vol. 108, pp. 221–225, 2019.
- [16] E. Lee *et al.*, "Performance analysis of the asymmetric dual-hop relay transmission with mixed RF/FSO links," *IEEE Photon. Technol. Lett.*, vol. 23, no. 21, pp. 1642–1644, 2011.
- [17] B. Ashrafzadeh *et al.*, "A framework on the performance analysis of dual-hop mixed FSO-RF cooperative systems," *IEEE Trans. on Commun.*, vol. 67, no. 7, pp. 4939–4954, 2019.
- [18] L. Yang *et al.*, "Performance analysis of dual-hop mixed PLC/RF communication systems," *IEEE Systems J.*, pp. 1–12, 2021.
- [19] I. Trigui *et al.*, "Shadowed FSO/mmWave systems with interference," *IEEE Trans. on Commun.*, vol. 67, no. 9, pp. 6256–6267, 2019.
- [20] Y. Zhang *et al.*, "On the performance of dual-hop systems over mixed FSO/mmWave fading channels," *IEEE Open J. of the Commun. Soc.*, vol. 1, pp. 477–489, 2020.
- [21] W. Gheeth *et al.*, "Performance analysis of integrated power-line/visible-light communication systems with AF relaying," in *2018 IEEE Global Commun. Conf. (GLOBECOM)*, 2018, pp. 1–6.
- [22] S. Li *et al.*, "Performance analysis of mixed RF-UWOC dual-hop transmission systems," *IEEE Trans. Veh. Technol.*, vol. 69, no. 11, pp. 14 043–14 048, Nov. 2020.
- [23] P. Ramirez-Espinosa *et al.*, "The α - κ - μ shadowed fading distribution: statistical characterization and applications," in *2019 IEEE Global Commun. Conf. (GLOBECOM)*, 2019, pp. 1–6.
- [24] E. N. Papatotiriou *et al.*, "A new look to THz wireless links: Fading modeling and capacity assessment," in *2021 IEEE 32nd Annu. Int. Symp. on Personal, Indoor and Mobile Radio Commun.*, 2021, pp. 1–6.
- [25] F. Yang, J. Cheng, and T. A. Tsiftsis, "Free-space optical communication with nonzero boresight pointing errors," *IEEE Transactions on Communications*, vol. 62, no. 2, pp. 713–725, 2014.
- [26] A. Kilbas, *H-Transforms: Theory and Applications*. CRC Press, 2004.
- [27] I. S. Gradshteyn and I. M. Ryzhik, *Table of Integrals, Series, and Products*. Academic press, San Diego, CA, 6th edition, 2000.
- [28] P. Mittal and K. Gupta, "An integral involving generalized function of two variables," *Proc. Indian Acad. Sci.*, vol. 75, no. 9, pp. 117–123, 1972.
- [29] E. Illi *et al.*, "A performance study of a hybrid 5G RF/FSO transmission system," in *2017 Int. Conf. on Wireless Netw. and Mobile Commun. (WINCOM)*, 2017, pp. 1–7.
- [30] P. Sen *et al.*, "The TeraNova platform: An integrated testbed for ultra-broadband wireless communications at true Terahertz frequencies," *Computer Networks, Elsevier*, 2020.